ELECTRODEPOSITION OF ZINC OXIDE FILMS FROM CHOLINE CHLORIDE BASED IONIC LIQUID MEDIA CONTAINING ZINC AND NITRATE IONS

Claudia-Sorina DUMITRU[1], Anca COJOCARU[2], Liana ANICAI[3], Adina COTARTA[4], Teodor VISAN[5]

The paper is focused on investigation of electrode processes during cathodic deposition of zinc oxide onto glassy carbon electrode from choline chloride-urea and choline chloride – ethylene glycol ionic liquids as solvents. Comparative cyclic voltammograms were recorded in the presence of single KNO_3 salt, single $Zn(NO_3)_2$ salt and KNO_3 + $Zn(NO_3)_2$ mixture. The irreversible process of NO_3^- reduction is catalysed by Zn^{2+} ions or metallic Zn first deposited. At very negative potentials and slow scan rate the mechanism consists in ZnO precipitation by a chemical reaction between Zn^{2+} and O^{2-} (or other oxide species produced by NO_3^- reduction) which needs time to be carried out.

Keywords: Zinc oxide, electrodeposition, cyclic voltammetry, zinc nitrate solutions, choline chloride based ionic liquids

1. Introduction

Zinc oxide (ZnO) is a II-VI semiconductor with a wide band gap of 3.37 eV at room temperature, which has attracted an interest in last years because its suitable energy-band structure and excellent properties such as optical, electronic and piezoelectric properties. Usual applications of ZnO powders are in the rubber industry, photocatalysis, sun-screenes, paints, varnishes, plastics and cosmetics. Films of ZnO possess several favorable properties, such as good transparency, high electron mobility, and room-temperature photoluminescence, used in emerging applications for liquid crystal displays, energy-saving or heat-protecting

[1] PhD student, Department of Inorganic Chemistry, Physical Chemistry and Electrochemistry, University POLITEHNICA of Bucharest, Romania
[2] Assoc. prof., Department of Inorganic Chemistry, Physical Chemistry and Electrochemistry, University POLITEHNICA of Bucharest, Romania, e-mail: anca.cojocaru@chimie.upb.ro
[3] 1-st degree Scientific Researcher, PhD, Center of Surface Science and Nanotechnology, University POLITEHNICA of Bucharest, Romania
[4] Prof., Department of Inorganic Chemistry, Physical Chemistry and Electrochemistry, University POLITEHNICA of Bucharest, Romania
[5] Prof., Department of Inorganic Chemistry, Physical Chemistry and Electrochemistry, University POLITEHNICA of Bucharest, Romania

windows, photovoltaic solar cells, gas sensors, ultrasonic oscillators, piezoelectric transducers, and in electronics as thin-film transistors, light-emitting diodes and laser diodes [1-10]. The literature shows that an optimum procedure to grow ZnO films without the need for subsequent annealing is electrodeposition, which has the advantages of low temperature (below 100^{o}C), soft processing of material and easily deposition of films on various substrate shapes, with controllable thickness.

The most studies for ZnO electrodeposition were carried out in aqueous hot solutions with different zinc salts, especially containing zinc nitrate [3,7,9,11-26]. As mechanism in electrolytes where $Zn(NO_3)_2$ is the sole precursor of both Zn^{2+} and NO_3^- ions it is generally accepted that the generation of hydroxide ion from cathodic reduction of NO_3^- ion is followed by a chemical precipitation of OH^- with Zn^{2+}, leading to $Zn(OH)_2$ formation in the vicinity of cathode surface. The simple chemical conversion as dehydration of $Zn(OH)_2$ into ZnO occurs in an ultimate step due to the temperature (50-90^{o}C) effect.

In the last years an innovative route to obtain nanocrystalline ZnO in the classical sol-gel synthesis has been developed by introducing as the morphological template an ionic liquid [27] instead of aqueous medium. Following this idea, Azaceta et al. [28,29] have selected 1-butyl-1-methylpyrrolidinium bis(trifluoromethanesulfonyl) imide (symbolized $PYR_{14}TFSI$) ionic liquid as reaction medium at 75-150^{o}C in view of producing ZnO films by cathodic deposition. In their first studies [28,29] the precursors were 5 mM $Zn(TFSI)_2$ salt and bubbled oxygen gas until saturation; a relatively soft thermal annealing (1 hour in air at 350^{o}C) to remove the ionic liquid was necessary to be performed. On cyclovoltammograms the reduction of O_2 was observed as a clear cathodic peak. The authors suggest a chemical reaction between the resulted O_2^- species (superoxide ion) with Zn^{2+} ions leading to ZnO precipitation; the process is electrochemically irreversible, so that no anodic current is detected on the anodic branch.

In a recent study [30], these authors have prepared hybrid ZnO films with a sponge morphology from the same $PYR_{14}TFSI$ ionic liquid, but using 50 mM $Zn(TFSI)_2$ and 30 mM N-butyl-N-methyl pyrrollidinium nitrate ($PYR_{14}NO_3$) as precursors for zinc cation and nitrate anion. On the cathodic branch of voltammograms a more pronounced cathodic wave was evidenced in the presence of both ions (Zn^{2+} and NO_3^-) than that for single $PYR_{14}NO_3$ dissolved salt, having a similar peak potential (-1.2 V vs. ferrocene couple) as in previous studies with bubbled oxygen. The increased peak current for NO_3^- reduction process is explained by an electrocatalysis effect due to presence of Zn^{2+}. The fast consumption of O_2^- superoxide species has led to increased rate of ZnO formation.

Doan et al. [31] prepared ZnO from an ionic liquid consisting in 1-butyl-1-methylpyrrolidinium bis(trifluoromethanesulfonyl)imide). They have electrodeposited firstly a metallic Zn film on colloidal crystal template, then

removed the template, and finally oxidized the Zn film in air at elevated temperature. Tulodziecki et al. [32] have reported a ZnO electrodeposition process at cathode in similar traditional ionic liquids, namely electrolytes based on methylimidazolium bis(trifluoromethylsulfonyl)imides: EMIMTFSI (1-ethyl derivate), BMPTFSI (1-butyl derivate) or BMIMTf (1-butyl-3-methylimidazolium (trifluoromethanesulfonate)), together with addition of a proper co-solvent to ionic liquid.

At present, ionic liquids based on quaternary ammonium salt such as choline chloride (2-hydroxy-ethyl-trimethyl ammonium chloride, ChCl) have gained a great attention and are recommended as *green alternative* for electrodeposition purposes. Such analogous ionic liquids consist in eutectic mixtures of ChCl with a hydrogen bond donor which may be urea, ethylene glycol, glycerine, malonic acid, citric acid or oxalic acid. These binary mixtures have melting points lower than room temperature, are cheaper and potentially recyclable, with no harm on human health. The cathodic electrodeposition of ZnO films in choline chloride - urea ionic liquid (commercial name Reline) was performed for the first time by Horiuti et al. [33]. Zinc perchlorate was the precursor for Zn^{2+} and bubbled oxygen was precursor for oxide ions; Mo/glass substrate was employed as the substrate for ZnO transparent film. Differential pulse voltammetry (DPV) was carried out and a cathodic peak attributed to the reduction of dissolved oxygen to superoxide was observed. The next step is a precipitation of ZnO. A successful electrochemical synthesis of ZnO nanopowders in ChCl-urea or in ChCl-ethylene glycol eutectic mixtures with addition of hydrogen peroxide was reported recently by us [34]. In order to precipitate ZnO, the anodic dissolution of metal zinc electrode was involved in that work.

To date, however, there were not published extensive studies regarding ZnO cathodic formation in ChCl based ionic liquids containing both Zn^{2+} and NO_3^- ions. The aim of this paper is to present a cyclic voltammetry study carried out to understand the cathodic mechanism of ZnO growth from the same choline chloride based ionic liquids, namely ChCl-urea and ChCl-ethylene glycol mixtures. To the best of our knowledge there is the first study regarding the electrodeposition at cathode of ZnO from such media. In this preliminary study we used the inert vitreous carbon (glassy carbon, GC) as working electrode which presents the necessary qualities to have a better insight into the deposition mechanism.

2. Reagents, materials and methods for investigation

The reagents were used as received. In order to prepare the eutectic (1:2 mole ratio) ionic liquids as solvents, choline chloride (99%, Sigma-Aldrich) was mixed with urea or ethylene glycol (both from Sigma-Aldrich) and heated in the

80-100^{o}C temperature range with gentle stirring until homogeneous, clear liquids were formed. To prepare the electrolytes with various concentrations of KNO_3 and $Zn(NO_3)_2.6H_2O$ the appropriate amounts of these precursors were dissolved and the solutions were heated again at 90^{o}C with permanent stirring. For comparison, in some experiments anhidrous $ZnCl_2$ (Fluka) was also used as precursor.

Cyclic voltammograms were recorded at different scanning rates (3-200 mV/s) by employing Biologic - SP 150 or Zahner elektrik IM 6e potentiostats. The temperature was maintained constant at 70^{o}C. The electrochemical cell contained a vitreous carbon disc (0.07 cm^2) as working electrode, a Pt larger plate as auxiliary electrode, and a Ag wire immersed in the ionic liquid as quasi-reference electrode. The working GC electrode was used as stationary or rotating electrode (500-5000 rpm). It was mechanically polished on a felt, cleaned successively with dilute HNO_3 solution, running water and distilled water and then dried before each measurement.

3. Results and discussion

Cyclic voltammetry (CV) was chosen as an appropriate electrochemical technique to evidence the cathodic formation of zinc oxide and the particular behavior of glassy carbon electrode in ionic liquids. As a strategy, the voltammetry experiments in Zn^{2+}-free ionic liquids containing KNO_3 were performed firstly, to determine the reduction potentials of NO_3^- species. Next, the main attention was paid to the electrode processes in ionic liquids which contain zinc nitrate as precursor for both Zn^{2+} and NO_3^- ions; correspondingly, the concentrations of investigated ions in these electrolytes have 1:2 molar ratio, according to stoichiometry of the salt. In the following step, studies of the electrolytes containing both zinc nitrate and potassium nitrate as dissolved salts allowed to determine the influence of increased nitrate ion concentration. In some experiments rotating disc electrode (RDE) was employed and in other cases, ionic liquids with dissolved $ZnCl_2$ salt were used in order to evidence the reduction potential of single Zn^{2+} ions.

3.1. Cyclic voltammetry in choline chloride – urea systems

Fig. 1 presents a family of CV curves recorded from 30 mM KNO_3 solution in ChCl-urea at 70^{o}C, applying various scan rates. The cathodic process representing the reduction of NO_3^- in this solution free of zinc ions starts at -1.5 V and reaches a peak located in the potential range from -1.8 to -2.2 V. The peak current increases linearly with square root of scan rate (not shown) thus proving a diffusion controlled process. Nevertheless, the gradual potential shift to more negative values of this peak with increased scan rate is an indication of a

quasireversible process from electrochemically point of view. It is worth to mention that both oxidation and reduction of NO_3^- were studied previously in a traditional ionic liquid based on methylimidazolium with dissolved 1-butyl-3-methylimidazolium nitrate as precursor [35].

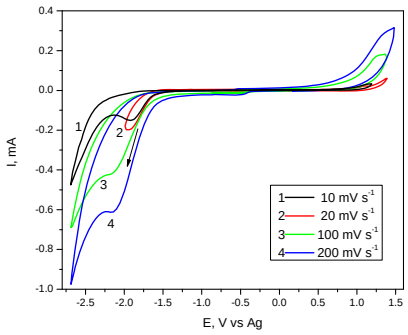

Fig. 1. CVs from ChCl-urea + 30 mM KNO_3 on GC electrode, 70 °C

Figs. 2 a-c show the voltammetric responses of GC electrode in three different electrolytes and a comparison of CV curves was made. It may be observed in Fig. 2a the couple of peaks for deposition/dissolution of metallic zinc where zinc ions are single species (from $ZnCl_2$ precursor). The main cathodic peak located at -1.4 V was attributed to Zn deposition and it has previously a wave (at -1.2 V) which may be due to an underpotential deposition of Zn, an usual process of metals deposited onto inert surface of electrode. The anodic peak at -0.9 V is sharp in shape being a characteristic feature to stripping of Zn from glassy carbon.

Fig. 2b presents comparatively CVs of a single nitrate salt (10 mM $Zn(NO_3)_2$) and two nitrate salts (10 mM $Zn(NO_3)_2$ + 50 mM KNO_3) dissolved in ChCl-urea ionic liquid solvent. For single dissolved $Zn(NO_3)_2$ an increase of current starts at -1.15 V and a cathodic peak appears at -1.28 V that is related to Zn metal deposition (curve 1). For more negative scanning, the continuous increase of current is attributed to NO_3^- reduction. Curve 2 refers to a solution where the total NO_3^- concentration (70 mM) becomes much more than of zinc ions (10 mM). So, the predominant reaction is now NO_3^- reduction with a cathodic peak at -2.15 V. Hence, the comparison of the two reduction processes shows an increase of peak current from 0.1 mA to 0.8 mA by supplementary introducing 50 mM NO_3^-.

In Fig. 2c the CVs were recorded from more concentrated solutions in Zn^{2+} ions (20 mM) and also a clear influence of Zn^{2+} presence is described. Curve 1 shows Zn metal deposition within -1.3 ÷ -1.6 V range followed by NO_3^- reduction. The peak current for NO_3^- reduction corresponding to single KNO_3 solution (curve 2) is lower around three times comparing to peak current for nitrate salts mixture (curve 3, the multiplication ratio of NO_3^- millimolar concentration becoming here 70:40). These results clearly demonstrate that zinc

ions have an electrocatalytic effect to NO_3^- reduction. It seems that this process is quite irreversible because the shift toward negative potential of NO_3^- reduction in the case of dissolved nitrate salts mixture. Also, on anodic branches of voltammograms no significant oxidation peak appears, except the peak at very positive potentials (1.2 V) attributed to oxidation of Cl^- ions leading to Cl_2 gas evolution.

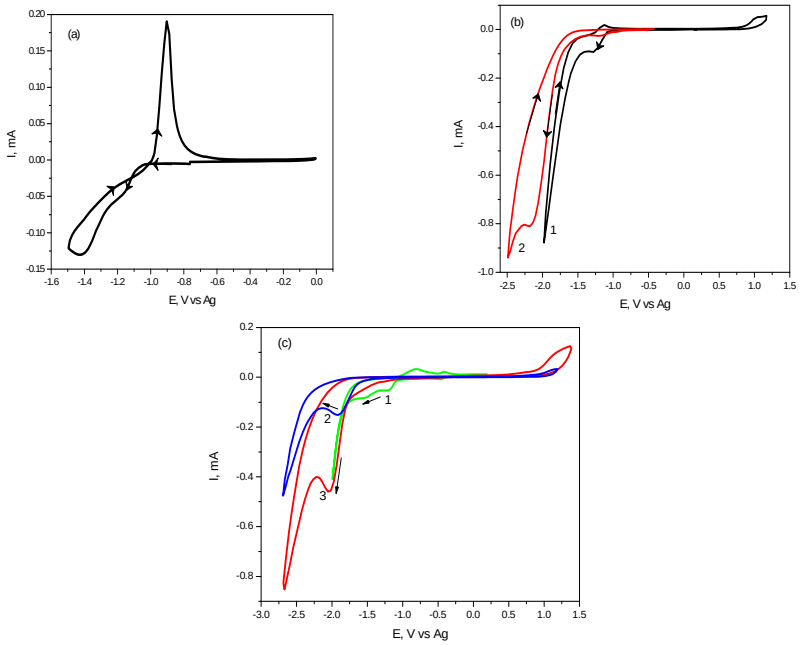

Fig. 2. Comparative CVs on GC electrode at 70 °C from ChCl-urea solvent with different dissolved salts: (a) 10 mM $ZnCl_2$, 5 mV/s; (b) 10 mM $Zn(NO_3)_2$ (curve 1) and 10 mM $Zn(NO_3)_2$ + 50 mM KNO_3 (curve 2), both at 20 mV/s; (c) 20 mM $Zn(NO_3)_2$, 20 mV/s (curve 1), 30 mM KNO_3, 10 mV/s (curve 2), and 20 mM $Zn(NO_3)_2$ + 30 mM KNO_3, 20 mV/s (curve 3)

The proposed mechanism of ZnO cathodic synthesis from ionic liquids takes into account the absence of water ions participation. Therefore the reduction of nitrate ions, which is the first step of EC mechanism, does not can produce hydroxide ions, but oxide ions are rather produced:

$$NO_3^- + 2\,e^- \rightarrow NO_2^- + O^{2-} \quad (1)$$

As Figs. 1 and 2c show, the reduction of nitrate ions into nitrite ions in solutions free of Zn^{2+} occurs effectively in a range of very negative potentials, extended sometimes even to -2.2 V. The larger overpotential for this reaction on GC than on Pt or other metallic surfaces is expected. In general the reduction of nitrate in ionic liquids (as in aqueous solutions, too) is not favorable from energetical point of view, because the reduction of an anion occurs on the cathode which is here a very smooth surface.

The second step in the mechanism is a direct precipitation of ZnO performed by coupling of Zn^{2+} with O^{2-} ions which just were formed by nitrate ions reduction:

$$Zn^{2+} + O^{2-} \rightarrow ZnO \downarrow \quad (2)$$

This pure chemical reaction is related to the lack of anodic peaks leading to the conclusion that that NO_3^- reduction is an irreversibile electrode process. Because of this precipitation reaction, the ZnO synthesis needs time to be carried out and this is probably connected to the favorable influence of low scan rates. On contrary, voltammograms with fast scan rate may lead to an incomplete conversion, so it is possible as some amount of Zn^{2+} to remain non-reacted and this may lead to Zn metal electrodeposition. This explains the very small anodic peaks (attributed to Zn metal stripping) occurred on curves 1 in Figs. 2b and 2c.

Alternative ways for above described EC-type mechanism can be proposed for ZnO formation by coupling the zinc ions with peroxide and superoxide ions which can also result by nitrate ion reduction [35]. The corresponding EC mechanism includes now an instable precipitate of either zinc peroxide (processes (3) and (4)) or zinc superoxide (processes (5) and (6) that break down rapidly in ZnO and molecular oxygen:

$$2NO_3^- + 2e^- \rightarrow 2NO_2^- + O_2^{2-} \quad (3)$$

$$Zn^{2+} + O_2^{2-} \rightarrow ZnO_2 \rightarrow ZnO\downarrow + 1/2\ O_2 \quad (4)$$

$$2NO_3^- + e^- \rightarrow 2NO_2^- + O_2^- \quad (5)$$

$$Zn^{2+} + 2O_2^- \rightarrow ZnO_4 \rightarrow ZnO\downarrow + 3/2\ O_2 \quad (6)$$

The influence of scan rate (v) to the shape of voltammograms recorded in 10 mM $Zn(NO_3)_2$ solution is shown in Figs. 3 a-e. When the scan rate is v=20 or 50 mV/s the usual behavior is observed (Figs. 2b,c), with a small current peak at direct scan that does not increase with v. This may be attributed to zinc metal deposition and it is followed by nitrate reduction and zinc oxide formation (processes (2), (4) and (6)). Less likely is another EC route comprising a further oxidation of just formed zinc metal by the following chemical reaction:

$$Zn + NO_3^- \rightarrow ZnO + NO_2^- \quad (7)$$

A plateau of current is also seen at backwards scan in the cathodic region followed by a small anodic peak of zinc metal stripping. On contrary, for fast scanning of potential (v=100 or 200 mV/s, Figs. 2d,e) a continuous increase of current is observed on direct scan which may be attributed to reaction (7). The cathodic plateau that appears only along the reverse scan may represent a new zinc deposition. In these cases the cathodic branches of voltammograms have two points of crossbreeding.

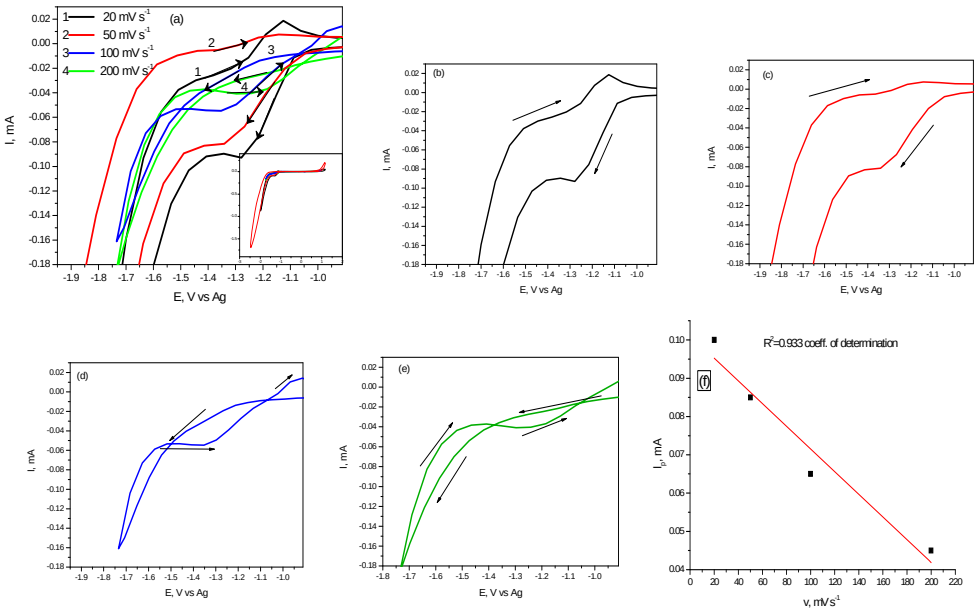

Fig. 3. (a) Zoom of CVs family from ChCl-urea + 10 mM $Zn(NO_3)_2$ on GC electrode , 70°C, with insertion showing electrode potential limits; (b-e) single CVs at 20, 50, 100 and 200 mV/s, respectively; (f) I_p-v linear dependence for the first cathodic peak attributed to zinc metal deposition

The favorable influence of slow scan rate for zinc oxide precipitation is explained by a kinetic limited process due to the complexity of the process, including final steps of conversion into zinc oxide. Surprinsingly, the peak potentials in all cases of zinc deposition remain constant (at -1.3 V) whether the scan is directly or reversed. Also, an unusual behavior for zinc deposition is the linear decreased dependence of peak current (I_p) with scan rate, shown in Fig. 3f. The straight line has the coefficient of determination of R^2=0.933 and a slope with the value of -2.9×10^{-4} mAs/mV.

The influence of various scan rates to the shape of voltammograms recorded in 20 mM $Zn(NO_3)_2$ + 30 mM KNO_3 solution with ChCl-urea solvent is shown in Fig. 4. This family of voltammograms is typical for an irreversible process which does not require nucleation overpotential, with a current of peak (recorded in forward direction) increasing with scan rate and a shift of this peak to more negative potentials. The final increase of cathodic current (the scan was extended to more negative than -2.5 V) is attributed to the reduction of cholinium cation originating from the ionic liquid solvent. It is possible for this process to be diffusion controlled.

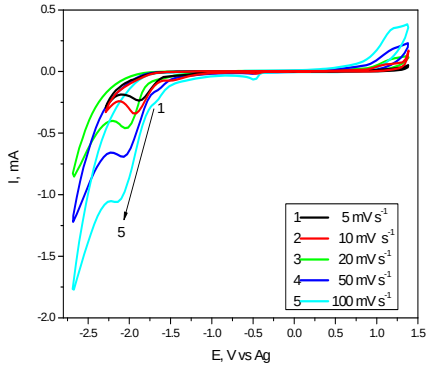

Fig. 4. CVs from ChCl-urea + 20 mM $Zn(NO_3)_2$ + 30 mM KNO_3 on GC electrode, 70°C, with different scan rates

Preliminary experiments were performed in ChCl-urea + 10 mM $Zn(NO_3)_2$ solution using rotating disc electrode (RDE) voltammetry technique. It is worth to mention that RDE voltammetry with glassy carbon electrodes used are reported for the first time in literature of zinc oxide formation in choline chloride based ionic liquids. The family of CV curves at constant rotation rate (500 rpm) together with details about single voltammograms is shown in Figs. 5. We selected in Fig. 5b only the cathodic portion which corresponds to the zinc metal deposition and its conversion into zinc oxide. As can be seen in Fig. 5c, at slow scan rate the cathodic current during forward scanning is lower compared to that from reverse scan. At fast scanning the current has an usual behavior, an example being given in Fig. 5d. On the whole, Figs. 5 suggest that the rotation of the disc electrode is favorable to zinc oxide formation, without cathodic peak occurrence as in the case of stationary electrode.

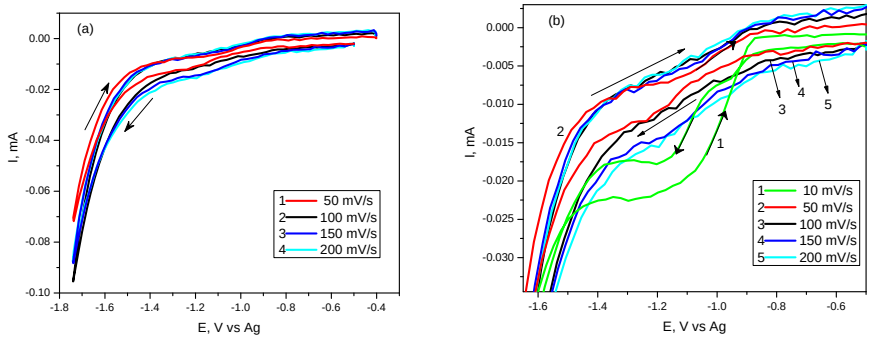

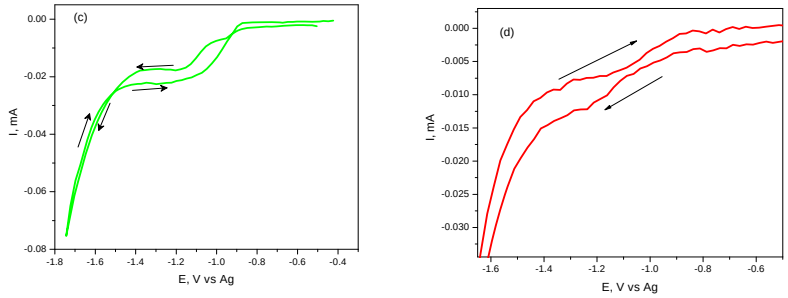

Fig. 5. (a,b) CVs from ChCl-urea + 10 mM $Zn(NO_3)_2$ on GC rotating electrode (RDE), 500 rpm, 70°C, at different scan rates;
(c) single CV, 10 mV/s; (d) single CV, 50 mV/s

In order to exhibit the influence of rotation rate of GC disc on the shape of CVs recorded from the same system at constant scan rate, we show comparatively RDE voltammograms recorded at low values of rotation per minute (Fig. 6a) and at high values of rpm (Fig. 6b), respectively. Except for very slow rotations (100 and 200 rpm) CV curves during the direct scan present almost identical plateaus of current, regardless rpm, in the potential range from -1.2 to -1.6 V. The process may be attributed to the EC route of zinc oxide formation *via* zinc metal deposition (reaction (7)); the current is constant regardless the amplitude of rotation. As the arrows show in Figs. 6, plateaus with higher limiting cathodic current (i_L) are recorded during the reverse scan. Metallic zinc deposit is supposed to be produced in this portion of cathodic current, followed by zinc stripping along to small anodic peak. Up to 5000 rpm we noticed a decrease of i_L with rotation rate, a dependence which is contrary to the Levich equation used in RDE voltammetry for mass-controlled processes.

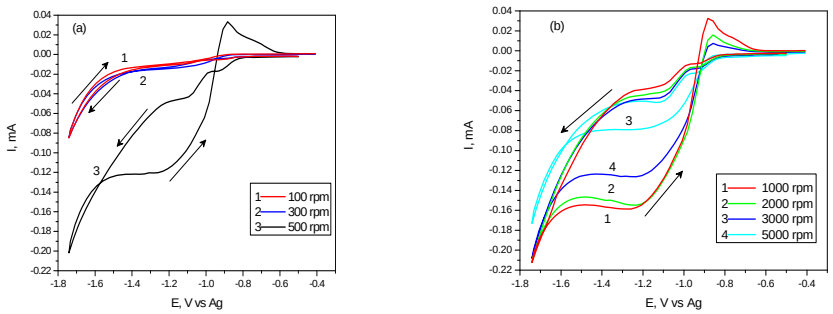

Fig. 6. CVs from ChCl-urea + 10 mM $Zn(NO_3)_2$ on GC rotating electrode (RDE), 70°C, 20 mV/s, at different rotation rates:
(a) 100; 300 and 500 rpm; (b) 1000; 2000; 3000 and 5000 rpm

3.2. Cyclic voltammetry in choline chloride – ethylene glycol systems

The study in choline chloride – ethylene glycol ionic liquid (commercial name Ethaline) was performed similarly as in choline chloride – urea mixture by using the same GC electrode and keeping a constant temperature, 70°C. Fig. 7 presents CV curves recorded from 30 mM KNO_3 solution in ChCl-EG by applying two rates of potential scan. The reduction of NO_3^- in this solution free of zinc species starts at -1.6 V and reaches a cathodic peak located in the potential range from -1.85 to -2 V.

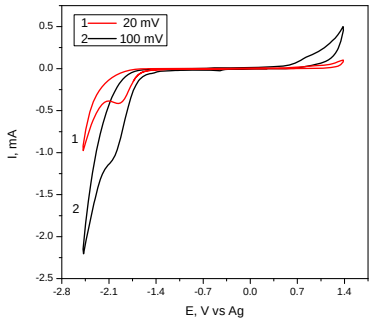

Fig. 7. CVs on GC electrode from ChCl-EG + 30 mM KNO_3, 70°C, at two scan rates: 20 mV/s (curve 1); 100 mV/s (curve 2)

Similar to the same process in ChCl-urea system, the peak current clearly increases with scan rate, being probably a I_p-$v^{1/2}$ dependence that would confirm a diffusion-controlled NO_3^- reduction. On the anodic branch of voltammogram there is no any anodic peak until continuous increase of current at very positive potentials, due to oxidation of Cl^- from ionic liquid solvent (similarly as in ChCl-urea solvent). Thus, the NO_3^- reduction in ChCl-EG may be considered an irreversible electrochemical process.

The voltammograms obtained in different cases of dissolved nitrates are shown in Figs. 8. A comparison between CV curves 1 and 2 in Fig. 8a demonstrates quite different cathodic processes: the peak at -1.3 V for single $Zn(NO_3)_2$ solution belongs to zinc deposition, whereas that at -1.9 V for single KNO_3 solution belongs to NO_3^- reduction. However, in the case of dissolved zinc precursor (curve 1) the second cathodic step after zinc deposition is also NO_3^- reduction at potentials more negative than -1.5 V which leads to ZnO formation. This fact explains the irreversible voltammetric behavior of $Zn(NO_3)_2$ solution.

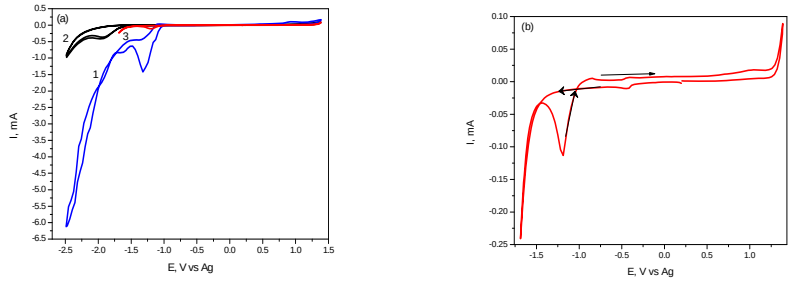

Fig. 8. (a) Comparative CVs on GC, 70°C, 20 mV/s, from ChCl-EG solvent with different dissolved nitrate salts: 20 mM $Zn(NO_3)_2$ (curve 1); 30 mM KNO_3 (curve 2); 20 mM $Zn(NO_3)_2$ + 30 mM KNO_3 (curve 3); (b) detailed curve 3 of CV response

Curve 3 for $Zn(NO_3)_2$ + KNO_3 solution from Fig. 8a (shown in detail in Fig. 8b, too) exhibits a non-usual route of cathodic branch. During the first scan the current increases just at more negative potentials than -1.5 V. The electrochemically generated O^{2-} ions (or O_2^{2-} and O_2^{-} ions) from nitrate ion reduction then react to Zn^{2+} producing zinc oxide by a route *via* processes (1) and (2) or alternatives discussed above, eqs. (3-6). Nevertheless, along the reverse scan only a clear cathodic peak located at -1.2 V is observed and it is attributed to metallic zinc deposit which is rapidly converted into ZnO according to eq. (7).

A series of CV curves obtained from ChCl-EG + 20 mM $Zn(NO_3)_2$ on GC stationary electrode is represented in Figs. 9. As detailed CVs show, a normal voltammetric response along the cathodic scan is observed at scan rates in the range of 5-20 mV/s, with a peak at about -1.4 V corresponding to Zn deposition at direct scan. By extending the scan at more negative potentials (up to -2.5 V in Fig. 9d) the nitrate ion reduction and precipitation step to form ZnO take place. Increasing the scan rate at 50 or 100 mV/s a change in voltammetric behavior is noticed, namely during direct scan the peak is diminished in its current (Fig. 9e) until total disappearance (Fig. 9f). Correspondingly, during the reverse scan a cathodic peak increasingly higher is observed which is attributed also to zinc deposition having a peak potential exactly with that for direct scan.

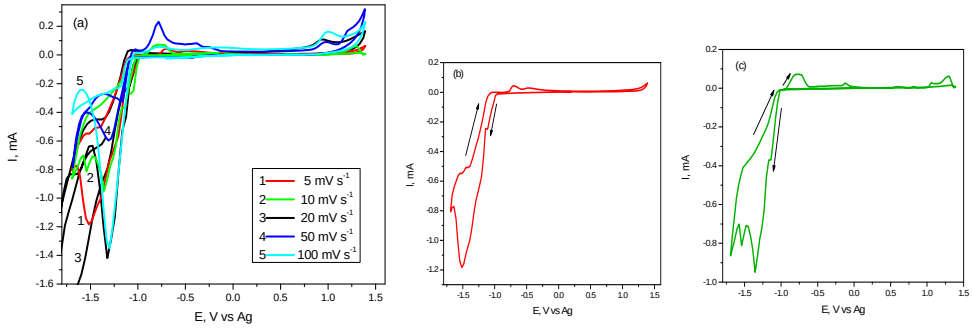

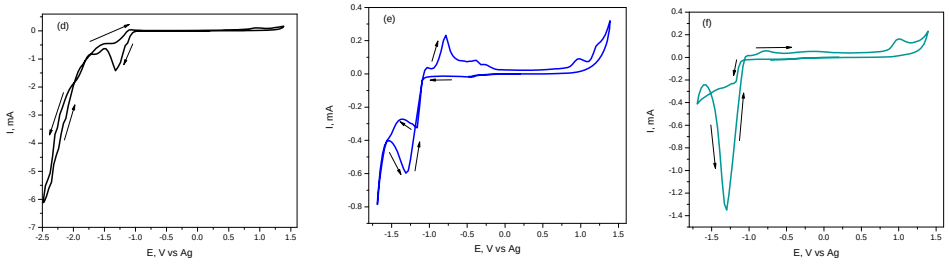

Fig. 9. (a) CVs from ChCl-EG + 20 mM $Zn(NO_3)_2$ on GC electrode, 70 ^oC;
(b-f) separate CV curves at scan rates: 5; 10; 20; 50; 100 mV/s, respectively

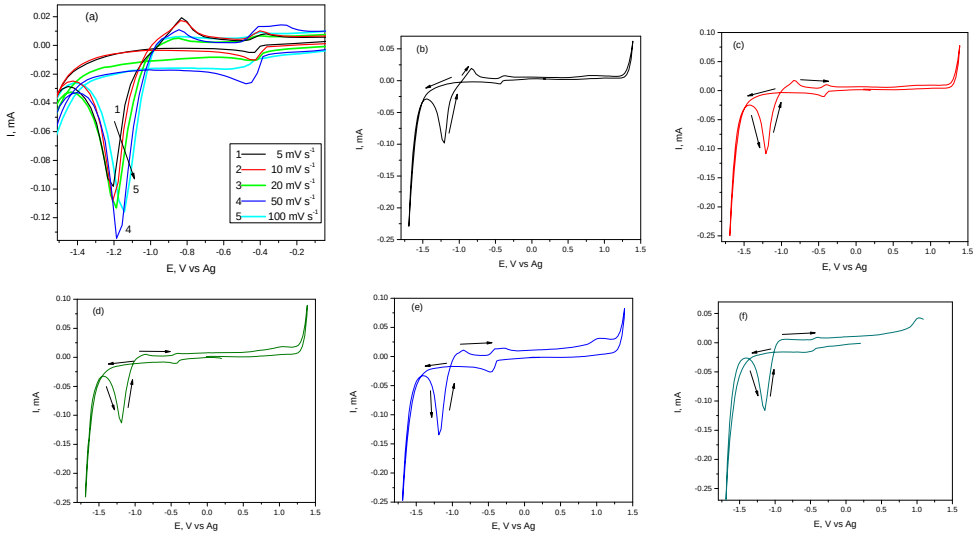

Fig. 10. (a) CVs from ChCl-EG + 20 mM $Zn(NO_3)_2$ + 30 mM KNO_3 on GC electrode, 70 ^oC, for different scan rates;
(b-f) separate CV curves for scan rates: 5; 10; 20; 50; 100 mV/s, respectively

Fig. 10 presents a family of voltammograms recorded from both dissolved nitrates in ChCl-EG ionic liquid solvent. In this case, by scanning toward negative potentials at any scan rate the formation of ZnO *via* processes (1-6) is supposed to be produced, due to continuous increase of current. A small peak at -0.4 V is probably an underpotential deposition of Zn metal, but its significance is not very important during the overall ZnO synthesis process. Similar to CVs from Figs. 9e and 9f, the reverse scan has led to the occurrence of a pronounced cathodic peak attributed to metallic Zn deposit which is also oxidized rapidly into ZnO at temperature of 70^oC. By comparing CVs from Figs. 9 and 10 it can deduce that the formation of ZnO is intensified in the system with both dissolved precursors for NO_3^-.

4. Conclusions

Investigations of cathodic deposition of zinc oxide onto glassy carbon from choline chloride - urea and choline chloride – ethylene glycol ionic liquids as solvents have shown that this process is very complex and may have different EC mechanisms at 70^{o}C. Cyclic voltammograms recorded in the presence of single KNO_3 salt demonstrated the existence of NO_3^- reduction which is an irreversible and diffusion-controlled process. In solutions with single $Zn(NO_3)_2$ salt the occurrence of metallic Zn deposit was evidenced, but also ZnO precipitate is formed especially during slow scanning. RDE voltammetry has shown a favorable influence of stirring. ZnO precipitate is produced in solutions with $KNO_3 + Zn(NO_3)_2$ mixture due to the excess of NO_3^- concentration. In both ionic liquids (ChCl-urea and ChCl-EG) the Zn^{2+} ions either were reduced to Zn metal or remained adsorbed onto electrode surface, playing in both cases the role of electrocatalyst for nitrate ion reduction.

Acknowledgements

Claudia-Sorina Dumitru is grateful for financial support from the European Social Fund through POSDRU /88/ 1.5/S/ 60203 Project. Part of this work was financially supported under M ERA Net Program, NANOCOATIL 7-082/2013 Research Project.

R E F E R E N C E S

1. *K.H. Yeo, L.K. The, C.C. Wong*, Process and characterization of macroporous periodic nanostructured zinc oxide via electrodeposition, J. Crystal Growth **287**, 2006, pp. 180–184.
2. *M. Sima, I. Enculescu, Ma. Sima, E. Vasile, T. Visan*, EIS studies of electrodeposition process of manganese and copper doped ZnO wires, Surf. Interf. Anal. **40**, 2008, pp. 561-565.
3. *S.K. Sharma, A. Rammohan, A. Sharma*, Templated one step electrodeposition of high aspect ratio n-type ZnO nanowire arrays, J. Colloid Interf. Sci. **344**, 2010, pp. 1–9.
4. *Ma. Sima, T. Visan, M. Sima, E. Vasile*, ZnO:Mn submicron wires prepared by electrochemical synthesis, UPB Sci. Bull., Series B **72** (1), 2010, pp. 27-35.
5. *Z. Zhang, G.W. Meng, Q.L. Xu, Y.M. Hu, Q. Wu, Z.J. Hu*, Aligned ZnO nanorods with tunable size and field emission on native Si substrate achieved via simple electrodeposition, J. Phys. Chem. C **114**, 2010, pp. 189-193.
6. *Ma. Sima, T. Visan, E. Matei, F. Ungureanu, I. Enculescu, M. Sima*, Electrochemical growth of eosine Y / manganese doped ZnO as hybrid films and nanowires, Z. Phys. Chem. **225**, 2011, pp. 325-339.
7. *X. Luo, L. Xu, B. Xu, F. Li*, Electrodeposition of zinc oxide/tetrasulfonated copper phthalocyanine hybrid thin film for dye-sensitized solar cell application, Appl. Surf. Sci. **257**, 2011, pp. 6908–6911.
8. *D. Chu, S. Li*, Growth and electrical properties of doped ZnO by electrochemical deposition, New J. Glass Ceram. **2** (1), 2012, 16977.

9. *H. Chettah, D. Abdi*, Effect of the electrochemical technique on nanocrystalline ZnO electrodeposition, its structural, morphological and photoelectrochemical properties, Thin Solid Films **537**, 2013, pp. 119–123.
10. *J. Li, H. Li, Y. Xue, H. Fang, W. Wang*, Facile electrodeposition of environment-friendly Cu_2O/ZnO heterojunction for robust photoelectrochemical biosensing, Sensors Actuators B **191**, 2014, pp. 619–624.
11. *S. Otani, J. Katayama, H. Umemoto, M. Matsuoka*, Effect of bath temperature on the electrodeposition mechanism of zinc oxide film from zinc nitrate solution, J. Electrochem. Soc. **153** (8), 2006, pp. C551-C556.
12. *T. Mahalingam, V.S. John, L.S. Hsu*, Microstructural analysis of electrodeposited zinc oxide thin films, J. New Mater. Electrochem. Syst. **10**, 2007, pp. 9-14.
13. *M. Sima, A.C. Manea, Ma. Sima, T. Visan*, Investigation by electrochemical impedance spectroscopy of electrodeposition of zinc-oxide microwires using nitrate by template method, Rev. Chim. (Bucharest) **58** (8), 2007, pp. 741-746.
14. *F. Peng, X.M. Li, X.D. Gao*, Transparent and compact zinc oxide thin films via two-step electrodeposition from aqueous solution, Key Eng. Mater. **336-338**, 2007, pp. 2221-2223.
15. *V. Georgieva, A. Tanusevski*, Some properties of zinc oxide thin films obtained by cathodic electrodeposition, AIP Conf. Proc. **899**, 2007, pp. 756.
16. *S.K. Park, Y.K. Lee, H.T. Kwak, C.R. Park, J. Park, Y.R. Do*, Periodic growth of ZnO nanorod arrays on two-dimensional SiN_x nanohole templates by electrochemical deposition, J. Phys. Chem. C **112**, 2008, pp. 4129-4133.
17. *J. Elias, R. Tena-Zaera, C. Levy-Clement*, Effect of the chemical nature of the anions on the electrodeposition of ZnO nanowire arrays, J. Phys. Chem. C **112**, 2008, pp. 5736-5741.
18. *A. Kathalingam, M.R. Kim, Y.S. Chae, J.K. Rhee, T. Mahalingam,* Studies on electrochemically deposited ZnO thin films, J. Korean Phys. Soc. **55** (6), 2009, pp. 2476-2481.
19. *C.V. Manzano, D. Alegre, O. Caballero-Calero, B. Alen, M.S. Martin-Gonzalez*, Synthesis and luminescence properties of electrodeposited ZnO films, J. Appl. Phys. **110**, 2011, 043638.
20. *S. Sun, S. Jiao, K. Zhang, D. Wang, S. Gao, H. Li, J. Wang, Q. Yu, F. Guo, L. Zhao*,
Nucleation effect and growth mechanism of ZnO nanostructures by electrodeposition from aqueous zinc nitrate baths, J. Crystal Growth **359**, 2012, pp. 15–19.
21. *L. Hu, J. Yan, M. Liao, H. Xiang, X. Gong, L. Zhang, X. Fang*, An optimized ultraviolet -A light photodetector with wide-range photoresponse based on ZnS/ZnO biaxial nanobelt, Adv. Mater. **24**, 2012, pp. 2305-2309.
22. *C. Dunkel, M. Wark, T. Oekermann, R. Ostermann, B.M. Smarsly*, Electrodeposition of zinc oxide on transparent conducting metal oxide nanofibers and its performance in dye sensitized solar cells, Electrochim. Acta **90**, 2013, pp. 375-381.
23. *N. Ait Ahmed, M. Eyraud, H. Hammache, F. Vacandio, S. Sam, N. Gabouze, P. Knauth, K. Pelzer, T. Djenizian*, New insight into the mechanism of cathodic electrodeposition of zinc oxide thin films onto vitreous carbon, Electrochim. Acta **94**, 2013, pp. 238–244.
24. *K. Zarebska, M. Kwiatkowski, M. Gniadek, M. Skompska*, Electrodeposition of $Zn(OH)_2$, ZnO thin films and nanosheet-like Zn seed layers and influence of their morphology on the growth of ZnO nanorods, Electrochim. Acta **98**, 2013, pp. 255–262.
25. *L. Wang, X. Zhu, J. Liu*, Study for the electrochemical deposition of ZnO nanocones
on Ti-Ni substrate and electrochemiluminescence, ECS J. Solid State Sci. Technol. **3** (4), 2014, pp. R50-R52.
26. *C.S. Dumitru, Ma. Sima, A. Cojocaru*, Electrochemical studies on the growth process of the zinc oxide films from nitrate solutions, Rev. Chim. (Bucharest) **65** (7), 2014, pp. 835-839.

27. *R. Rajiv Gandhi, S. Gowri, J. Suresh, M. Sundrarajan*, Ionic liquids assisted synthesis of ZnO nanostructures: Controlled size, morphology and antibacterial properties, J. Mater. Sci. Technol. **29**, 2013, pp. 533-538.
28. *E. Azaceta, R. Tena-Zaera, R. Marcilla, S. Fantini, J. Echeberria, J.A. Pomposo, H. Grande, D. Mecerreyes*, Electrochemical deposition of ZnO in a room temperature ionic liquid: 1-butyl-1-methylpyrrolidinium bis(trifluoromethane sulfonyl)imide, Electrochem. Commun. **11**, 2009, pp. 2184–2186.
29. *E. Azaceta, R. Marcilla, D. Mecerreyes, M. Ungureanu, A. Dev, T. Voss, S. Fantini, H.J. Grande, G. Cabanero, R. Tena-Zaera*, Electrochemical reduction of O_2 in 1-butyl-1-methylpyrrolidinium bis(trifluoromethanesulfonyl) imide ionic liquid containing Zn^{2+} cations: deposition of non-polar oriented ZnO nanocrystalline films, Phys. Chem. Chem. Phys. **13**, 2011, pp. 13433-13440.
30. *E. Azaceta, J. Idigoras, J. Echeberria, A. Zukal, L. Kavan, O. Miguel, H.J. Grande, J.A. Anta, R. Tena-Zaera*, ZnO–ionic liquid hybrid films: electrochemical synthesis and application in dye-sensitized solar cells, J. Mater. Chem. A **1**, 2013, pp. 10173–10183.
31. *M. Tulodziecki, J.-M. Tarascon, P.L. Taberna, C. Guéry*, Electrodeposition growth of oriented ZnO deposits in ionic liquid media, J. Electrochem. Soc. **159** (12), 2012, pp. D691-D698.
32. *N. Doan, T. Vainikka, E.-L. Rautama, K. Kontturi, C. Johans*, Electrodeposition of macroporous Zn and ZnO films from ionic liquids, Int. J. Electrochem. Sci. **7**, 2012, pp. 12034-12044.
33. *M. Harati, D. Love, W.M. Lau, Z. Ding*, Preparation of crystalline zinc oxide films by one-step electrodeposition in Reline, Mater. Lett. **89**, 2012, pp. 339–342.
34. *S. Costovici, A. Petica, C.S. Dumitru, A. Cojocaru, L. Anicai*, Electrochemical synthesis of ZnO nanopowder involving choline chloride based ionic liquids, Chem. Eng. Trans. **41**, 2014, pp. 343-348.
35. *T.L. Broder, D.S. Silvester, L. Aldous, C. Hardacre, A. Crossley, R.G. Compton*, The electrochemical oxidation and reduction of nitrate ions in the room temperature ionic liquid [C2Mim][NTf2]; the latter behaves as a 'melt' rather than an 'organic solvent', New J. Chem. **31** (6), 2007, pp. 966-972.
36. *A.S. Catrangiu, A. Cotarta, A. Cojocaru, T. Visan*, Diffusion-controlled electrode processes of Sb^{3+} and Cu^{2+} in ionic liquids containing choline chloride, UPB Sci. Bull., Series B, in press.